Cont 8909022--20

CONF-890902--20

DE90 001079

# THE STUDY OF EXOTIC N≈82 NUCLEI USING THE DARESBURY RECOIL MASS SEPARATOR


J. H. McNeill[1,2]

Oak Ridge National Laboratory and Joint Institute of Heavy-Ion Research
Oak Ridge, TN 37831, U.S.A.; Department of Physics
Schuster Laboratory, University of Manchester
Manchester, M13 9PL, England, U.K.

A. A. Chishti, W. Gelletly[3], M. A. C. Hotchkis, and B. J. Varley

Department of Physics, Schuster Laboratory
University of Manchester, Manchester, M13 9PL, England, U.K.

J. Blomqvist

Manne Siegbahn Institute of Physics, S-10405 Stockholm, Sweden

P. J. Daly

Department of Chemistry, Purdue University
West Lafayette, Indiana 47907, U.S.A.

M. Piiparinen

Department of Physics, Jyväskylä University, SF-40100 Jyväskylä, Finland

P. J. Woods

Department of Physics, University of Edinburgh
EH9 3JZ, Scotland, U.K.


## ABSTRACT


Experiments using the Daresbury Recoil Mass Separator have identified microsecond isomers in the exotic N=82, 83 nuclei $^{153}$Yb, $^{153}$Lu, $^{154}$Lu, and $^{154}$Hf, and have established their decay schemes. The results for $^{153}$Lu and $^{154}$Hf, together with those for lighter N=82 isotones, provide an outstanding illustration

of the dependence of E2 transition rates between $j^n$ states on the subshell occupation, and demonstrate that half-filling of the $\pi h_{11/2}$ subshell in the N=82 series occurs just below Z=71 $^{153}$Lu. The result of the isomer in the even-odd N=83 nucleus $^{153}$Yb shows that the isomerism is due to a low-energy E2 transition rather than an E3 transition as in lighter N=83 even-odd isotones, which is another consequence of the $\pi h_{11/2}$ subshell being about half-filled. Furthermore, the long-lived isomer observed in the odd-odd N=83 nucleus $^{154}$Lu also reflects that the $\pi h_{11/2}$ subshell is close to being half-filled.

## I. FILLING OF THE $\pi h_{11/2}$ SUBSHELL: N=82 ISOTONES $^{153}$Lu AND $^{154}$Hf

Some ten years ago it was found [1] that the Z=64, N=82 species $^{146}$Gd displays properties resembling those of a doubly magic nucleus. This discovery stimulated spectroscopic studies of many neighbouring nuclei which have a few valence nucleons outside the $^{146}$Gd core and may be well described in terms of shell model configurations. Particularly interesting are the proton-rich N=82 isotones above $^{146}$Gd, where the three nearly degenerate proton subshells $h_{11/2}$, $s_{1/2}$ and $d_{3/2}$ are being filled. The high-j unique parity $\pi h_{11/2}$ orbitals should be especially important in the formation of high-spin states, and one could expect yrast excitations of the type $\pi h_{11/2}{}^n$ to figure prominently in the spectra of N=82 isotones with Z-64 valence protons. Experiments [2-7] have identified and characterized the decays of related $\pi h_{11/2}{}^n$ E2 isomers below 3 MeV in the 2 to 6 valence proton N=82 nuclei $^{148}$Dy, $^{149}$Ho, $^{150}$Er, $^{151}$Tm and $^{152}$Yb (Figure 1). In the even-A nuclei the isomeric transitions are between $10^+$ and $8^+$ $\pi h_{11/2}{}^n$ states of seniority v=2; in the odd-A nuclei they are

$27/2^- \rightarrow 23/2^-$ transitions between $\pi h_{11/2}{}^n$ v=3 states. These isomeric decays also populate $3^-$ octupole, $[\pi h_{11/2}{}^{n-1} s_{1/2}]5^-$ and $[\pi h_{11/2}{}^{n-1} d_{3/2}]7^-$ v=2 excitations in the even-A nuclei, and corresponding $15/2^+$, $19/2^+$ and $23/2^+$ v=3 states, formed by coupling with an additional $h_{11/2}$ proton, in the odd-A nuclei.

The results for $^{148}$Dy include a complete spectrum [2] of $\pi h_{11/2}{}^2$ levels ($0^+$, $2^+$, $4^+$, $6^+$, $8^+$, $10^+$) whose energies provide empirical two-body matrix elements for calculating the $\pi h_{11/2}{}^n$ spectra in the heavier isotones. Moreover, Lawson [8] has used the $^{148}$Dy energies to show that the condition for no seniority mixing is very nearly fulfilled. When seniority is a good quantum number, the reduced E2 transition rates between corresponding $\pi h_{11/2}{}^n$ states of the same seniority should be proportional to $(6-n)^2$, where n is the $\pi h_{11/2}$ occupation number, and should become zero when n=6 at the half filled subshell [9, 10]. The relevant expressions for the v=2 and v=3 transitions are [8]:

$$B(E2;\ 10^+ \rightarrow 8^+) = \left[\frac{6-n}{4}\right]^2 \frac{2025}{35321\pi} \cdot (e_{eff} \langle r^2 \rangle)^2$$

and

$$B(E2;\ 27/2^- \rightarrow 23/2^-) = \left[\frac{6-n}{3}\right]^2 \cdot \frac{32400}{265837\pi} \ (e_{eff} \langle r^2 \rangle)^2.$$

Using the fixed value for the effective charge $e_{eff} = 1.52e$, and $\langle r^2 \rangle = 32\ fm^2$ for the $\pi h_{11/2}$ orbital, the measured B(E2) values for the five N=82 nuclei are very well reproduced [11,12] (Figure 2) <u>by assuming that in every case n equals Z-64, the number of valence protons</u>. For $^{152}$Yb with 6 valence protons, the experimental B(E2) is not exactly zero as in the ideal picture, but its very small value (0.02 Weisskopf units) demonstrates that the $\pi h_{11/2}$ subshell is close to being half-filled in the $8^+$ and $10^+$ states.

It is difficult to see why this simple model is so successful, since one would expect that in the relevant states of the $Z > 67$ nuclei, the $s_{1/2}$ and $d_{3/2}$ subshells should also be partly occupied by proton pairs, reducing the occupation of $\pi h_{11/2}$. On the other hand, the single particle energy gap at Z=64 is significantly smaller than the gaps at traditional magic numbers, and scattering of proton pairs from $g_{7/2}$ or $d_{5/2}$ across the gap into $h_{11/2}$ may compensate in some measure for the depletion into $s_{1/2}$ and $d_{3/2}$. Calculations [11,13] which take account of these two effects suggest that half-filling of the $\pi h_{11/2}$ subshell might be postponed to $^{153}_{71}Lu_{82}$ or $^{154}_{72}Hf_{82}$, but there have been no data for these nuclei up to now.

The N=82 isotones $^{153}Lu$ and $^{154}Hf$ lie very close to the proton drip line. Previous attempts to study these nuclei have been unfruitful mainly because they can be produced only in reactions with very low cross sections. In the present experiments, the sensitivity for detection of weak isomeric decays was considerably enhanced by the use of the Daresbury Recoil Mass Separator [14]. The ionization chamber, normally located behind the separator focal plane, was replaced by an aluminium catcher foil which was surrounded by four large Ge detectors and a LEPS. Fusion-evaporation product recoils from the reaction $^{102}Pd + ^{54}Fe \rightarrow ^{156}Hf^*$ were mass analyzed, and, after passing through the position-sensitive focal plane detector [14], were deposited on the catcher foil for $\gamma$-ray measurements. Time relationships between signals from the position-sensitive detector and from the $\gamma$-ray detectors were used for mass, half-life and $\gamma\gamma$ coincidence determinations. Since the separator transit time is ~1 μs, only long-lived isomeric species were observed, but they could be studied under low background conditions. The measurements were performed over a three day period using 10 to 15 particle nA beams of 240 to 245 MeV $^{54}Fe$ ions on a 1 mg/cm$^2$ $^{102}Pd$ target.

Production cross-sections predicted by the code CASCADE [15] for the reaction products $^{153}Yb$, $^{153}Lu$, $^{154}Lu$, and $^{154}Hf$, all of which were expected to have long-lived isomers, are summarized in Table I, which also lists relative yields at the catcher foil for the isomeric species identified in these experiments. In line with the predictions, by far the strongest family of γ-rays was observed in the A=153 mass window (Figure 7) and to be coincident with Yb x-rays. The 23 γ-rays thus assigned to $^{153}Yb$ have been placed [16] in the decay scheme (Figure 9) of a new 15 μs isomer in that nucleus. A second, much weaker (<2%) γ-ray family, including 130, 174 and 217 keV lines, was also observed in the A=153 mass window. These γ-rays are assigned to the p2n evaporation product $^{153}Lu$, because they appeared in coincidence with Lu K x-rays (Figure 3a), whereas the $^{153}Yb$ lines were suppressed by more than a factor of 50 in the same spectrum. Other transitions in $^{153}Lu$ were identified by γγ coincidences (for example Figure 3b). The $^{153}Lu$ γ-rays were observed to decay

$$T_{1/2} = 15 \pm 3\ \mu s,$$

and they are all placed in the isomeric decay scheme shown in Figure 4 on the basis of the γγ coincidence results. Table II lists the energies and intensities for all γ-rays placed in the $^{153}Lu$ decay scheme. Spins and parities are assigned mainly by analogy with the similar decay schemes of the shorter-lived $27/2^-$ isomers [3,4,6] in $^{149}Ho$ and $^{151}Tm$. The total conversion coefficient of the 130 keV transition

$$\alpha_{tot}\ (130\ \text{keV}) = 1.1 \pm 0.2$$

derived from intensity balance, is consistent with E2 character, and the measured half-life gives:

$$B(E2;\ 130\ keV,\ {}^{153}Lu) = 0.45 \pm 0.09\ e^2fm^4,$$

the smallest value determined in the N=82 series. The $\gamma\gamma$ time distributions for $^{153}$Lu indicated a lower isomer with $T_{1/2} > 0.1$ μs, that we associate with the $23/2^-$ state.

As Figure 4 shows, the spectrum of $\pi h_{11/2}{}^7$ levels calculated using the empirical $\pi h_{11/2}{}^2$ interactions from $^{148}$Dy is in very good agreement with experiment, especially for the four topmost levels. The $21/2^-$ level in $^{153}$Lu, populated by an unobserved 21 keV transition from the $23/2^-$ level, has no observed counterparts in $^{149}$Ho and $^{151}$Tm. Theory [8] predicts such a level ~26 keV below the $23/2^-$ in each of the three nuclei, but the $23/2^- \rightarrow 21/2^-$ M1 transition is strongly forbidden. It appears that the $23/2^- \rightarrow 19/2^-$ E2 decay must be extremely retarded, as it is in $^{153}$Lu, before the $23/2^- \rightarrow 21/2^-$ transition becomes competitive. An interesting note is that the $27/2^-$ 15 μs isomeric state in $^{153}$Lu has a positive Q-value of 3.3 ± 0.7 MeV (Reference [17]) for proton decay to the $^{152}$Yb ground state, but this decay mode must be suppressed by the centrifugal barrier associated with $\ell = 13$ nucleon transfer and by the complicated nucleon rearrangements involved.

The possible A=154 products of the reaction were $^{154}$Yb, $^{154}$Lu, and $^{154}$Hf, and of these the N=84 nucleus $^{154}$Yb has no microsecond isomers. The most intense A=154 $\gamma$-rays were found to be coincident with Lu x-rays, and they are assigned [18] to a new 35 μs isomer in $^{154}$Lu (Figures 10 and 11). Careful scrutiny of the A=154 $\gamma$-ray spectrum for a possible $^{154}$Hf $2^+ \rightarrow 0^+$ transition in the

1490 to 1530 keV range suggested by systematics revealed a weak 1513 keV $\gamma$-ray that decayed with the half-life

$$T_{1/2} = 9 \pm 4 \ \mu s.$$

A gate on the 1513 keV transition (Figure 3c) indicated coincidence peaks (each with 4 to 6 counts) at 135, 214 and 311 keV, and additional gates on these low energy lines identified another $\gamma$-ray of 498 keV in the same nucleus (Figure 3d). Although the data are statistically poor and provide no Z-identification, the firm A=154 mass determination, the N=82 systematics and the observed reaction yield (Table I) all favour the assignment of these five $\gamma$-rays to the decay of a 9 $\mu$s isomer in $^{154}$Hf. When the transitions are ordered as shown in Figure 5, the smooth energy level systematics [2-7] of the even-A N=82 isotones are extended to Z=72 in a convincing manner. The value of the $^{152}$Yb $10^+$ half-life shown in Figure 5 was determined during the present studies. By assuming that the energies of the unobserved $10^+ \rightarrow 8^+$ E2 transitions in $^{152}$Yb and $^{154}$Hf lie within the range 14 to 70 keV, as systematics indicate, the following results are obtained:

$$B(E2;\ 10^+ \rightarrow 8^+,\ ^{152}Yb) = 0.9 \pm 0.1\ e^2fm^4$$

and

$$B(E2;\ 10^+ \rightarrow 8^+,\ ^{154}Hf) = 2.9 \pm 1.4\ e^2fm^4.$$

The faster transition rate for $^{154}$Hf is a clear signal that in this nucleus the $\pi h_{11/2}$ subshell is more than half-filled.

For both $^{153}$Lu and $^{154}$Hf, the B(E2) results are much smaller than the values predicted using the equations and model assumptions specified earlier, and they imply that the $\pi h_{11/2}$ occupation numbers for these nuclei are in fact somewhat less than Z-64. The overall results are illustrated in Figure 6, where the transition amplitudes $\sqrt{B(E2)}$ for the seven N=82 isotones are plotted versus

Z-64. The square root leaves an ambiguity about the sign of the E2 matrix element, which should change at the point of half-filling, but the data strongly indicate that the sign change occurs just before Lu. The fact that the smooth curves through the data points both intersect the zero axis at the same value of Z-64 provides reassurance that correct signs have been chosen for the amplitudes. The variation of E2 transition amplitude with number of valence protons is not exactly linear, but nearly so, and it is clear that the $\pi h_{11/2}$ subshell is closest to being half-filled in the Z=71 isotone $^{153}$Lu. It is less easy to specify the magnitude of the $\pi h_{11/2}$ E2 effective charge in this region, but it may be significantly larger [11] than 1.52e, the value suggested previously [2].

## II. THE 15 μs ISOMER IN THE Z=70, N=83 NUCLEUS $^{153}$Yb

An intriguing problem in the structure of proton-rich N=83 isotones has recently come to light [19]. Three-particle $27/2^-$ isomers, having the aligned configuration $(\pi h_{11/2}{}^{n})_{10}\nu f_{7/2}$, are well established [2,20,21] in the Z=66, 68 isotones $^{149}$Dy and $^{151}$Er. The main decay in each case is by a retarded low-energy E3 transition to a $21/2^+$ state of dominant $\pi h_{11/2}{}^{n-1} d_{3/2} \nu f_{7/2}$ character (Figure 8). Consequently, the isomeric half-lives are unusually long (~0.5s), so much so that Barden et al. [19] were able to study the competitive β-decay branching from the $27/2^-$ isomers to levels in N=84 daughter nuclei. However, when these workers went on to search for an analogous long-lived isomer in the Z=70 isotone $^{153}$Yb, they found none, and concluded that no $27/2^-$ E3 isomer exists in that nucleus [19].

The observation of the strong $^{153}$Yb γ-rays, which were observed to decay with the half-life

$$T_{1/2} = 15 \pm 1\ \mu s,$$

elucidates the systematics of proton-rich N=83 nuclei discussed in the previous paragraph. Comprehensive $\gamma\gamma$ coincidence results allowed us to place all the observed $^{153}$Yb $\gamma$-rays in the level scheme in Figure 9, and Table III lists the energies and intensities for all the $\gamma$-rays known to follow the decay of the $^{153}$Yb 15 $\mu$s isomer. Total conversion coefficients for low-energy transitions, determined from intensity balance requirements, yielded key information about multipolarities. The strong 51 keV transition is determined to have the total conversion coefficient value

$$\alpha_{tot}(51\ \text{keV}) = 0.49 \pm 0.06$$

which is indicative of E1 character. From an intensity balance condition with the 234 and 328 keV $\gamma$-rays, the conversion coefficient for the 97 keV transition is calculated to be

$$\alpha_{tot}(97\ \text{keV}) = 3.86 \pm 0.04,$$

indicating M1 character. However, some unobservable weak feeding from the assigned $19/2^+$ and $21/2^+$ levels into the $19/2^-$ level could occur and then the determined above conversion coefficient value is slightly too large, which would then suggest either M1 or E2 character. The 107 and 110 keV transitions are found to have the total conversion coefficient values:

$$\alpha_{tot}(107\ \text{keV}) = 2.81 \pm 0.04$$

and

$$\alpha_{tot}(110\ \text{keV}) = 2.5 \pm 0.2,$$

which indicate M1, and E2 or M1 character, respectively. Since no measurable lifetime was observed for the 110 keV transition, the E2 possibility may be discounted. On the basis of this information, together with the measured branching intensities and the N=83 systematics, spin-parity values are assigned with confidence (Figure 9).

The half-life of the 1202 keV level, interpreted as a $13/2^+$ state of $\nu i_{13/2} \times 3^-$ character, has been determined to be ~6 ns. The energy reduced branching to the 567 keV and ground states of $^{153}$Yb is almost identical to the known M2/E3 branching from the $13/2^+$ isomer in $^{151}$Er to the $\nu h_{9/2}$ and $\nu f_{7/2}$ single particle states (Figure 8). We note in passing that measurements of radioactivity from the catcher showed 567 keV $\gamma$-rays coincident with 511 keV annihilation radiation, indicating that the radioisotope $^{153}$Lu mainly $\beta^+$-decays by the expected fast Gamow-Teller transition $\pi h_{11/2} \rightarrow \nu h_{9/2}$.

From systematics, the strongly populated $15/2^+$, $17/2^+$ and $19/2^+$, $21/2^+$ levels in $^{153}$Yb are interpreted as members of $\pi h_{11/2}{}^{n-1} s_{1/2} \nu f_{7/2}$ and $\pi h_{11/2}{}^{n-1} d_{3/2} \nu f_{7/2}$ multiplets. The intense $21/2^+ \rightarrow 19/2^+$ 23 keV M1 was not detected, but it is clearly indicated by the coincidence results. The $21/2^+$ level is fed by the strong 51 keV E1 from a $23/2^-$ level that is assigned to the coupling of a $[\pi h_{11/2}{}^n]$ $8^+$ with $\nu f_{7/2}$. This level also deexcites through a $23/2^- \rightarrow 19/2^- \rightarrow 15/2^-$ cascade where the 97 and 329 keV transition energies closely resemble known $8^+ \rightarrow 6^+ \rightarrow 4^+$ spacings between $\pi h_{11/2}{}^n$ states in N=82 nuclei such as $^{148}$Dy and $^{150}$Er. Furthermore, the 1460 as well as the 1491 keV transition energies resemble the interpreted $\pi h_{11/2}{}^n$ $2^+ \rightarrow 0^+$ spacing in $^{152}$Yb. The 15 $\mu$s isomeric state almost certainly has the aligned configuration $[\pi h_{11/2}{}^n \nu f_{7/2}]27/2^-$. The $27/2^- \rightarrow 23/2^-$ isomeric transition was not observed; our measurements place an upper limit of 50 keV on its energy, and the deduced B(E2) is ~2 $e^2fm^4$. This transition, like the $\pi h_{11/2}{}^n$ $10^+ \rightarrow 8^+$ E2 transition in $^{152}$Yb, is highly retarded because in these nuclei the $\pi h_{11/2}$ subshell is close to being half-filled [7,12].

The present study thus provides a solution to the N=83 systematics problem outlined above. As Barden et al. [19] have discussed, the long-lived E3 isomers occur in $^{149}$Dy and $^{151}$Er because the strongly attractive neutron-proton interaction in the $\pi h_{11/2}\nu f_{7/2}$ $9^+$ coupling lowers the $\pi h_{11/2}{}^n\nu f_{7/2}$ $27/2^-$ aligned state below the $23/2^-$ multiplet member. With increasing Z, the n-p attraction diminishes as the half-filled $\pi h_{11/2}$ subshell is approached, and one consequence is that in $^{153}$Yb the $23/2^-$ is now found below the $27/2^-$ state, giving rise to E2 rather than E3 isomerism. The structure of other multiplets observed in $^{153}$Yb are also influenced by the reduced n-p interaction.

## III. THE 35 μs ISOMER IN THE Z=71, N=83 NUCLEUS $^{154}$Lu

As was discussed previously in Sections I and II, $27/2^-$ isomers of $\pi h_{11/2}{}^n$ v=3 character occur at ~2.7 MeV in the proton-rich N=82 isotones $^{149}$Ho, $^{151}$Tm and $^{153}$Lu. As both Z and the $\pi h_{11/2}$ occupation number increases, the observed $B(E2; 27/2^- \rightarrow 23/2^-)$ decreases sharply, reaching a value of only 0.45 $e^2fm^4$ (or 0.01 Wu) in $^{153}$Lu, where the $\pi h_{11/2}$ subshell is approximately half-filled. Corresponding $[\pi h_{11/2}{}^n\nu f_{7/2}]17^+$ isomers have been located [22,23] in the N=83 neighbouring nuclei $^{150}$Ho and $^{152}$Tm. Echoing the trend in the N=82 series, the $B(E2; 17^+ \rightarrow 15^+)$ diminishes from $^{150}$Ho to $^{152}$Tm, and by extrapolation a $17^+$ half-life much longer than 1 μs has been predicted [23] for the $^{154}$Lu isotone, which has not been studied up to now.

For the recent experiment discussed in Section I, the strongest family of γ-rays observed in the A=154 mass window was found to be coincident with Lu x-rays and therefore assigned to the pn evaporation product $^{154}$Lu. The isomeric half-life was determined to be:

$$T_{1/2} = 35 \pm 3 \text{ μs}.$$

Although the yield of the $^{154}Lu$ isomer at the catcher foil was only 4% of the $^{153}Yb$ isomeric yield, the $^{154}Lu$ $\gamma\gamma$ coincidence data recorded were of excellent quality, as is illustrated in Figure 10.

The 130 keV transition was found to be in prompt coincidence with all the other $^{154}Lu$ $\gamma$-rays (Figure 10a), and its total conversion coefficient was determined from intensity balance to be

$$\alpha_{tot}(130 \text{ keV}, {}^{154}Lu) = 1.14 \pm 0.21$$

in agreement with the theoretical E2 value. Accordingly, it is interpreted as the isomeric $17^+ \rightarrow 15^+$ transition. A key result, illustrated in Figure 10b, was the identification of the 130, 350, 678 and 1402 keV $\gamma$-ray cascade which closely resembles established $17^+ \rightarrow 15^+ \rightarrow 13^+ \rightarrow 11^+ \rightarrow 9^+$ E2 cascades in the $^{150}Ho$ and $^{152}Tm$ isotones [23]. All the strong $^{154}Lu$ $\gamma$-rays, except the 678 and 1402 keV lines, appeared in coincidence with the 215 keV transition (Figure 10c).

The $^{154}Lu$ isomeric decay scheme shown in Figure 11 is based on the comprehensive $\gamma\gamma$ coincidence results and on N=83 level systematics, and Table IV lists the energies and intensities for all the $\gamma$-rays that follow the decay of the $^{154}Lu$ 35 $\mu s$ isomer. Particularly, the spin-parity and suggested configuration assignments rest largely on systematic arguments. The $\pi h_{11/2}{}^{n}\nu f_{7/2}$ assignment for the two lowest $^{154}Lu$ levels extends a regular trend observed in the $^{148}Tb$, $^{150}Ho$ and $^{152}Tm$ isotones where the $8^+$ multiplet members are found 315, 217 and 114 keV, respectively, above the $[\pi h_{11/2}{}^{n}\nu f_{7/2}]$ $9^+$ ground states. The decay patterns of the $9^+_2$ and $10^+$ levels in $^{154}Lu$ support their interpretation as $\pi h_{11/2}{}^{n}\nu h_{9/2}$ states, corresponding to similar states identified in $^{152}Tm$ [23]; the lower energies in $^{154}Lu$ are consistent with the established downward trend in the $\nu h_{9/2}$ single particle energy with increasing Z. The $11^-$, $12^-$ and higher-lying negative parity $^{154}Lu$ levels are also probable counterparts of known excitations in $^{150}$Ho and $^{152}$Tm, and in most respects the three isomeric decays resemble one another closely. However, the 350 keV $\gamma$-ray in $^{154}$Lu is unlikely to be the $15^+ \rightarrow 13^+$ transition, as we first assumed. Such an E2 transition between $\pi h_{11/2}{}^n \nu f_{7/2}$ states would be so slow in this nucleus that the parent level should be isomeric, but the measurements revealed no intermediate isomers in the level scheme. A further difficulty would be the implied $15^+ \rightarrow 13^-$ assignment for the 520 keV transition. The most plausible solution is indicated in Figure 11, where an unobserved low-energy $15^+ \rightarrow 14^+$ M1 transition is followed by 350 keV $14^+ \rightarrow 13^+$ and 520 keV $14^+ \rightarrow 13^-$ decay branches in a manner consistent with the coincidence results. In the corresponding portion of the $^{153}$Lu level spectrum, the $\pi h_{11/2}{}^n$ $23/2^-$ state is isomeric, even though the $21/2^-$ state lies below it [18]; this happens because the $23/2^- \rightarrow 21/2^-$ M1 transition is forbidden within the $\pi h_{11/2}{}^n$ configuration. However, in $^{154}$Lu the $15^+ \rightarrow 14^+$ transition between $\pi h_{11/2}{}^n \nu f_{7/2}$ states can be fast, and may thus carry the entire decay intensity.

While the Figure 11 level scheme may not be correct in all details, there seems little doubt about the interpretation of the 130 keV E2 as the expected $17^+ \rightarrow 15^+$ isomeric transition. The measured half-life gives

$$B(E2;\ 130\ \text{keV},\ ^{154}\text{Lu}) = 0.19 \pm 0.02\ e^2\text{fm}^4,$$

much smaller than the values 182 ± 18 and 44 ± 2 $e^2$fm$^4$ determined from the anal $17^+ \rightarrow 15^+$ decays in $^{150}$Ho and $^{152}$Tm. Following Reference [23], we plot in Figu 12 the isomeric E2 transition amplitudes, $\sqrt{B(E2)}$, for N=82, 83 nuclei as a func tion of Z, with the assumption that the amplitude has changed sign only in $^{153}$Lu. The variation of $\sqrt{B(E2)}$ with Z is seen to be appropriate linear for eac set of the isotones. The shift in Figure 12 between the N=82 and N=83 lines ma be attributed to the $(\pi h_{11/2}{}^n)_{27/2} \nu f_{7/2}$ components of the $15^+$ states, which giv rise to similar contributions to the $17^+ \rightarrow 15^+$ transition amplitudes in each of the N=83 isotones. As mentioned above, this result has been anticipated in Reference [23], where a B(E2; $17^+ \rightarrow 15^+$) very close to zero was predicted for $^{154}$Lu

[1]Oak Ridge National Laboratory is operated by Martin Marietta Energy Systems, Inc., under Contract No. DE-AC05-84OR21400 with the U.S. Department of Energy.

[2]Present address: Oak Ridge National Laboratory, Oak Ridge, Tennessee 37831, U.S.A.

[3]Present address: SERC-Daresbury Laboratory, Daresbury, Warrington, Cheshire, WA4 4AD, England, U.K.

## ACKNOWLEDGMENTS

We thank R. Broda and C. J. Lister for useful discussions. We also thank G. Reed from the University of Manchester and the Daresbury Laboratory staff for technical assistance, and also special thanks go to D. Blunt for the making of the targets. This work has been funded by the U.K. Science and Engineering Research Council, during the period of which the first author, J. H. McNeill, was a postdoctoral research associate at the University of Manchester. The co-authors P. J. Daly and M. Piiparinen acknowledge support from the U.S. Department of Energy, and M. Piiparinen also acknowledges support from the Academy of Finland.

## REFERENCES


1. P. Kleinheinz, M. Ogawa, R. Broda, P. J. Daly, D. Haenni, H. Beuscher, and A. Kleinrahm, Z. Phys. A286, 27 (1978).

2. P. J. Daly, P. Kleinheinz, R. Broda, S. Lunardi, H. Backe, and J. Blomqvist, Z. Phys. A298, 173 (1980).

3. J. Wilson, S. R. Faber, P. J. Daly, I. Ahmad, J. Borggreen, P. Chowdhury, T. L. Khoo, R. D. Lawson, R. K. Smither, and J. Blomqvist, Z. Phys. A296, 185 (1980).

4. H. Helppi, Y. H. Chung, P. J. Daly, S. R. Faber, A. Pakkanen, I. Ahmad, P. Chowdhury, Z. W. Grabowski, T. L. Khoo, R. D. Lawson, and J. Blomqvist, Phys. Lett. 115B, 11 (1982); K. S. Toth, D. C. Sousa, J. M. Nitschke, and P. A. Wilmarth, Phys. Rev. C35, 620 (1987).

5. Y. H. Chung, P. J. Daly, H. Helppi, R. Broda, Z. W. Grabowski, M. Kortelahti, J. McNeill, A. Pakkanen, P. Chowdhury, R. V. F. Janssens, T. L. Khoo, and J. Blomqvist, Phys. Rev. C29, 2153 (1984).

6. J. H. McNeill, Ph.D. Thesis, Purdue University, 1986.

7. E. Nolte, G. Korschinek, and Ch. Setzensack, Z. Phys. A309, 33 (1982); E. Nolte, S. Z. Gui, G. Colombo, G. Korschinek, and K. Eskola, Z. Phys. A306, 223 (1982).

8. R. D. Lawson, Z. Phys. A303, 51 (1981).

9. A. de Shalit and I. Talmi, Nuclear Shell Theory (Academic, New York, 1963).

10. R. D. Lawson, Theory of the Nuclear Shell Model (Clarendon, Oxford, 1980).

11. J. Blomqvist, Int. Rev. of Nucl. Phys. 2 (World Scientific, Signapore, 1984) pp. 1-32.

12. P. J. Daly, Y. H. Chung, Z. W. Grabowski, H. Helppi, M. Kortelahti, P. Chowdhury, R. V. F. Janssens, T. L. Khoo, R. D. Lawson, and J. Blomqvist, in Proceedings of the International Conference on Nuclear Physics, Florence, 1, 73 (1983).

13. R. R. Chasman, Phys. Rev. C28, 1374 (1983).

14. A. N. James, T. P. Morrison, K. L. Ying, K. A. Connell, H. G. Price, and J. Simpson, Nucl. Inst. Meth. A267, 144 (1988).

15. F. Pühlhofer, Nucl. Phys. A280, 267 (1977).

16. J. H. McNeill, A. A. Chishti, P. J. Daly, M. A. C. Hotchkis, M. Piiparinen, and B. J. Varley, Z. Phys. A332, 105 (1989).

REFERENCES CONTINUED


17. Evaluated using ground state masses from A. H. Wapstra and G. Audi, Nucl. Phys. A432, 1 (1985).

18. J. H. McNeill, J. Blomqvist, A. A. Chishti, P. J. Daly, W. Gelletly, M. A. C. Hotchkis, M. Piiparinen, B. J. Varley, and P. J. Woods, to be published.

19. R. Barden, A. Plochocki, D. Schardt, B. Rubio, M. Ogawa, P. Kleinheinz, R. Kirchner, O. Klepper, and J. Blomqvist, Z. Phys. A329, 11 (1988).

20. A. M. Stefanini, P. J. Daly, P. Kleinheinz, M. R. Maier, and R. Wagner, Nucl. Phys. A258, 34 (1976); A. M. Stefanini, P. Kleinheinz, and M. R. Maier, Phys. Lett. 62B, 405 (1976).

21. J. Jastrzebski, R. Kossakowski, J. Lukasiak, M. Moszynski, Z. Preibisz, S. Andre, J. Genevey, A. Gizon, and J. Gizon, Phys. Lett. 97B, 50 (1980).

22. J. Wilson, Y. H. Chung, S. R. Faber, A. Pakkanen, P. J. Daly, I. Ahmad, P. Chowdhury, T. L. Khoo, R. D. Lawson, and R. K. Smither, Phys. Lett. 103B, 413 (1981).

23. J. McNeill, R. Broda, Y. H. Chung, P. J. Daly, Z. W. Grabowski, H. Helppi, M. Kortelahti, R. V. F. Janssens, T. L. Khoo, R. D. Lawson, D. C. Radford, and J. Blomqvist, Z. Phys. A325, 27 (1986).

Table I. Production cross-sections for the reaction $^{102}Pd + ^{54}Fe \rightarrow ^{156}Hf^*$ predicted by the code CASCADE at $^{54}Fe$ beam energies of 235 and 245 MeV. The right hand column gives relative experimental yields (in arbitrary units) for the isomeric species identified.

| Exit Channel | Product | σ(235 MeV) (mb) | σ(245 MeV) (mb) | Isomeric Yields* |
|---|---|---|---|---|
| 2pn | $^{153}Yb$ | 73 | 60 | 70 |
| p2n | $^{153}Lu$ | 2 | 3.5 | 1.0 |
| pn | $^{154}Lu$ | 3 | 1.2 | 2.5 |
| 2n | $^{154}Hf$ | 0.2 | 0.1 | 0.06 |

*Uncorrected for differences in the separator transmission for different products.

Table II. Energies, intensities, and placements of γ-rays following the 15 μs isomer in $^{153}$Lu.

| Energy (keV) | Off-Beam Intensity | Placements (keV) |
|---|---|---|
| 130.4(2) | 54(4) | 2633.0 |
| 174.0(2) | 46(4) | 1606.1 |
| 216.5(2) | 65(6) | 1822.6 |
| 270.0(3) | 24(2) | 2147.2 |
| 291.0(3) | 8(2)[a] | 2502.6 |
| 323.9(3) | 10(2)[a] | 2147.2 |
| 355.4(3) | 57(4) | 2502.6 |
| 389.1(3) | 35(3) | 2211.7 |
| 658.8(3) | 22(3) | 2481.4 |
| 715.1(3) | 35(4) | 2147.2 |
| 1432.1(3) | 100(9) | 1432.1 |
| 1606.1(3) | ~2 | 1601.1 |

[a] Obtained from coincidence gates.

Table III. Energies, intensities, and placements of γ-rays following the 15 μs isomer in $^{153}$Yb.

| Energy (keV) | Off-Beam Intensity | Placement (keV) |
|---|---|---|
| 50.8(2) | 765(76) | 2577.9 |
| 96.8(2) | 50(4) | 2577.9 |
| 107.2(2) | 67(4) | 2137.2 |
| 109.5(2) | 98(5) | 2246.7 |
| 234.4(2) | 226(11) | 2481.1 |
| 257.6(2) | 616(31) | 2504.3 |
| 267.7(2) | 90(4) | 2030.0 |
| 271.7(4) | 6(1) | 1762.3 |
| 280.5(3) | 12(2) | 2527.1 |
| 303.0(2) | 44(4) | 1762.3 |
| 328.4(3) | 17(2) | 2481.1 |
| 367.1(2) | 384(19) | 2504.3 |
| 539.4(2) | 142(7) | 2030.0 |
| 561.0(2) | 41(4) | 1762.3 |
| 566.7(2) | 189(9) | 566.7 |
| 635.1(2) | 160(8) | 1201.4 |
| 935.8(2) | 473(24) | 2137.2 |
| 951.2(3) | 13(2) | 2152.7 |
| 1045.3(2) | 612(31) | 2246.7 |
| 1196.0(3) | 22(2) | 1762.3 |
| 1201.4(2) | 1000(50) | 1201.4 |
| 1459.0(2) | 47(4) | 1459.0 |
| 1490.6(2) | 148(7) | 1490.6 |

Table IV. Energies, intensities, and placements of $\gamma$-rays following the 35 $\mu s$ isomer in $^{154}Lu$.

| Energy (keV) | Off-Beam Intensity | Placement (keV) |
|---|---|---|
| 98.0(6) | 7(4) | 1911.6 |
| 130.4(3) | 72(7) | 2561.5+x |
| 206.8(4) | 18(2) | 2431.1 |
| 215.4(3) | 100(10) | 1440.5 |
| 313.4(5) | 10(2) | 2224.3 |
| 316.2(5) | 9(2) | 1202.5 |
| 335.9(3) | 75(8) | 357.3 |
| 338.7(4) | 39(4) | 1225.1 |
| 350.0(3) | 99(10) | 2431.1 |
| 358.1(6) | 5(2) | 358.1 |
| 411.6(5) | 10(2) | 1813.9 |
| 470.7(4) | 31(3) | 1911.6 |
| 519.5(4) | 37(4) | 2431.1 |
| 529.1(4) | 34(5) | 886.4 |
| 640.6(4) | 70(7) | 2081.1 |
| 678.8(4) | 18(3) | 2081.1 |
| 784.3(6) | 8(2) | 2224.3 |
| 845.2(4) | 43(4) | 1202.5 |
| 1202.5(5) | 50(9) | 1202.5 |
| 1402.3(4) | 31(3) | 1402.3 |

FIGURE CAPTIONS

Figure 1. Systematics of the yrast levels up to 3 MeV in the N=82 isotones $^{148}$Dy, $^{149}$Ho, $^{150}$Er, $^{151}$Tm and $^{152}$Yb.

Figure 2. The E2 transition rates between $10^+$ and $8^+$ states of the $\pi h_{11/2}{}^n$ v=2 spectra in the even-A nuclei ($^{148}$Dy, $^{150}$Er, $^{152}$Yb) and those between $27/2^-$ and $23/2^-$ states of the $\pi h_{11/2}{}^n$ v=3 spectra in the odd-A nuclei ($^{149}$Ho, $^{151}$Tm). The measured B(E2)'s are shown with error bars, and the error bar for $^{152}$Yb is within the plotted point. Two parabolae show the calculated B(E2) transition rates of pure $\pi h_{11/2}{}^n$ configurations using $\langle e_{eff} r^2 \rangle \; \pi h_{11/2} = 49$ efm$^2$.

Figure 3. a)-d) Key γ-ray coincidence spectra for the specified mass windows and gating transitions.

Figure 4. Isomeric decay scheme for $^{153}$Lu. Transition arrow widths are proportional to the measured intensities, with internal conversion contributions unshaded. The calculated $\pi h_{11/2}{}^7$ spectrum, with the $27/2^-$ level energy matched to experiment, is shown to the left.

Figure 5. Energy systematics of even-A N=82 isotones, showing the main decay pathways of the $10^+$ isomers.

Figure 6. Measured E2 transition amplitudes for v=2 and v=3 isomeric transitions in N=82 isotones as a function of Z-64. Where error bars are not shown, they lie within the plotted point.

Figure 7. Off-beam γ-ray spectrum for A=153 mass recoils following the reaction $^{102}$Pd + 240-245 MeV $^{54}$Fe. Lifetime data are shown in the inset.

Figure 8. Systematics observed in the even-odd N=83 isotones $^{149}$Dy and $^{151}$Er.

Figure 9. The $^{153}$Yb level scheme. Arrow widths are proportional to the transiton intensities, with internal conversion contributions unshaded.

FIGURE CAPTIONS CONTINUED

Figure 10. a)-c) Key γ-ray coincidence spectra for transitions in $^{154}$Lu. Lifetime data are shown in the inset.

Figure 11. The $^{154}$Lu level scheme. Arrow widths are proportional to the transition intensities with internal conversion contributions unshaded.

Figure 12. Measured E2 transition amplitudes for v=3 and v=4 isomeric transitions in N=82 and N=83 isotones as a function of Z. Where error bars are not shown, they lie within the plotted point.

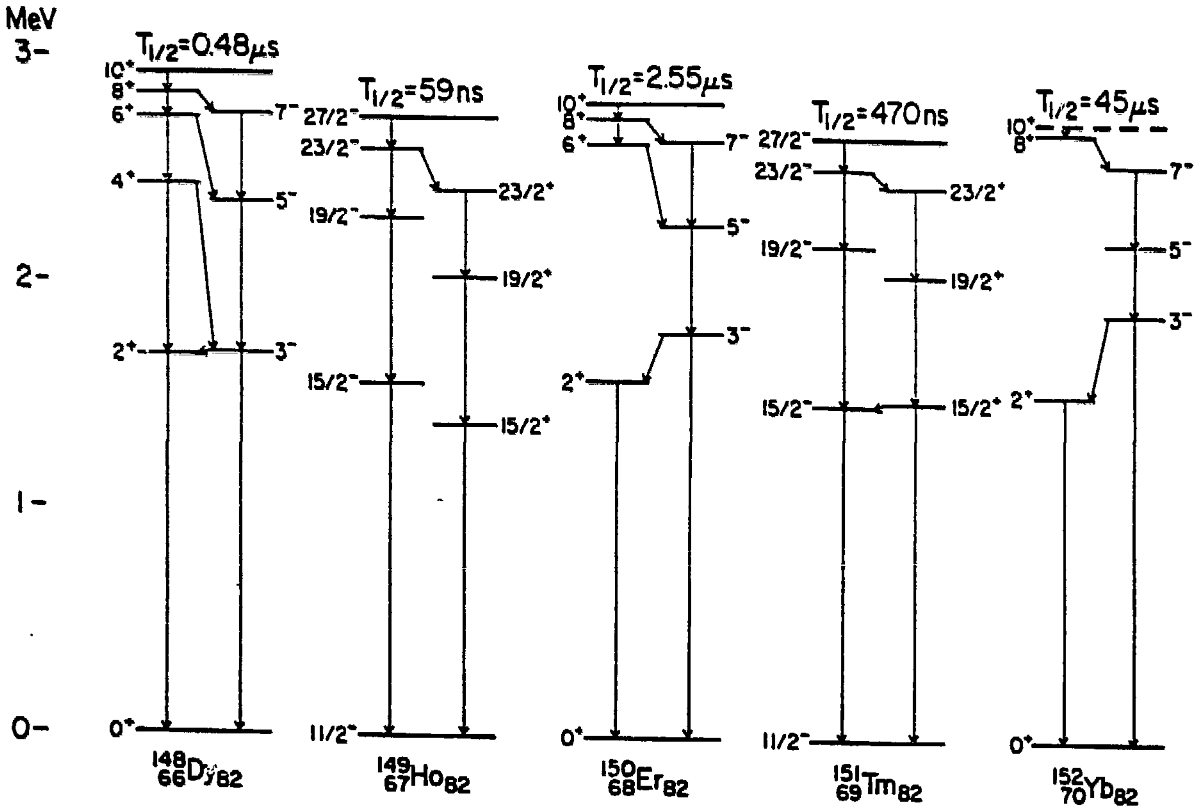
MeV
3-
2-
1-
0-
T1/2=0.48μs
10+
8+
6+
4+
2+
0+
7-
5-
3-
148 66 Dy 82
T1/2=59ns
27/2-
23/2-
19/2-
15/2-
11/2-
23/2+
19/2+
15/2+
149 67 Ho 82
T1/2=2.55μs
10+
8+
6+
2+
0+
7-
5-
3-
150 68 Er 82
T1/2=470ns
27/2-
23/2-
19/2-
15/2-
11/2-
23/2+
19/2+
15/2+
151 69 Tm 82
T1/2=45μs
10+
8+
2+
0+
7-
5-
3-
152 70 Yb 82

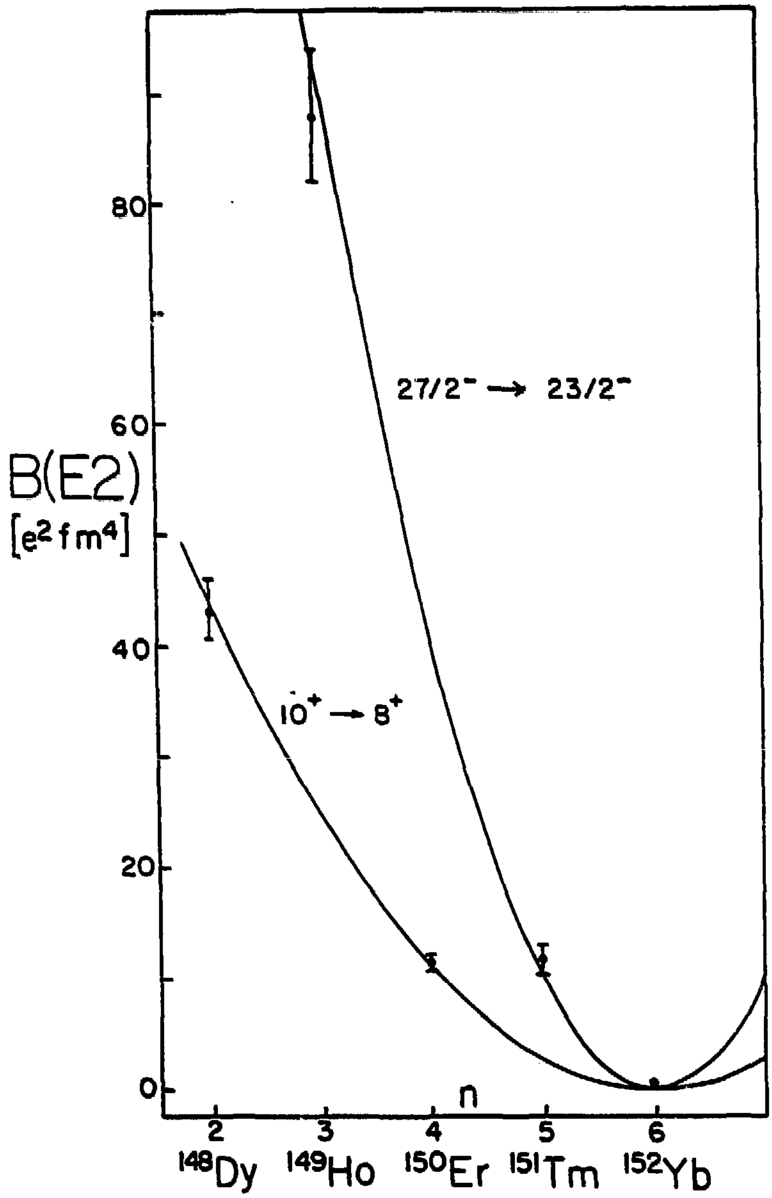
B(E2)
[e2 fm4]
80
60
40
20
0
27/2⁻ → 23/2⁻
10⁺ → 8⁺
n
2
3
4
5
6
148Dy
149Ho
150Er
151Tm
152Yb

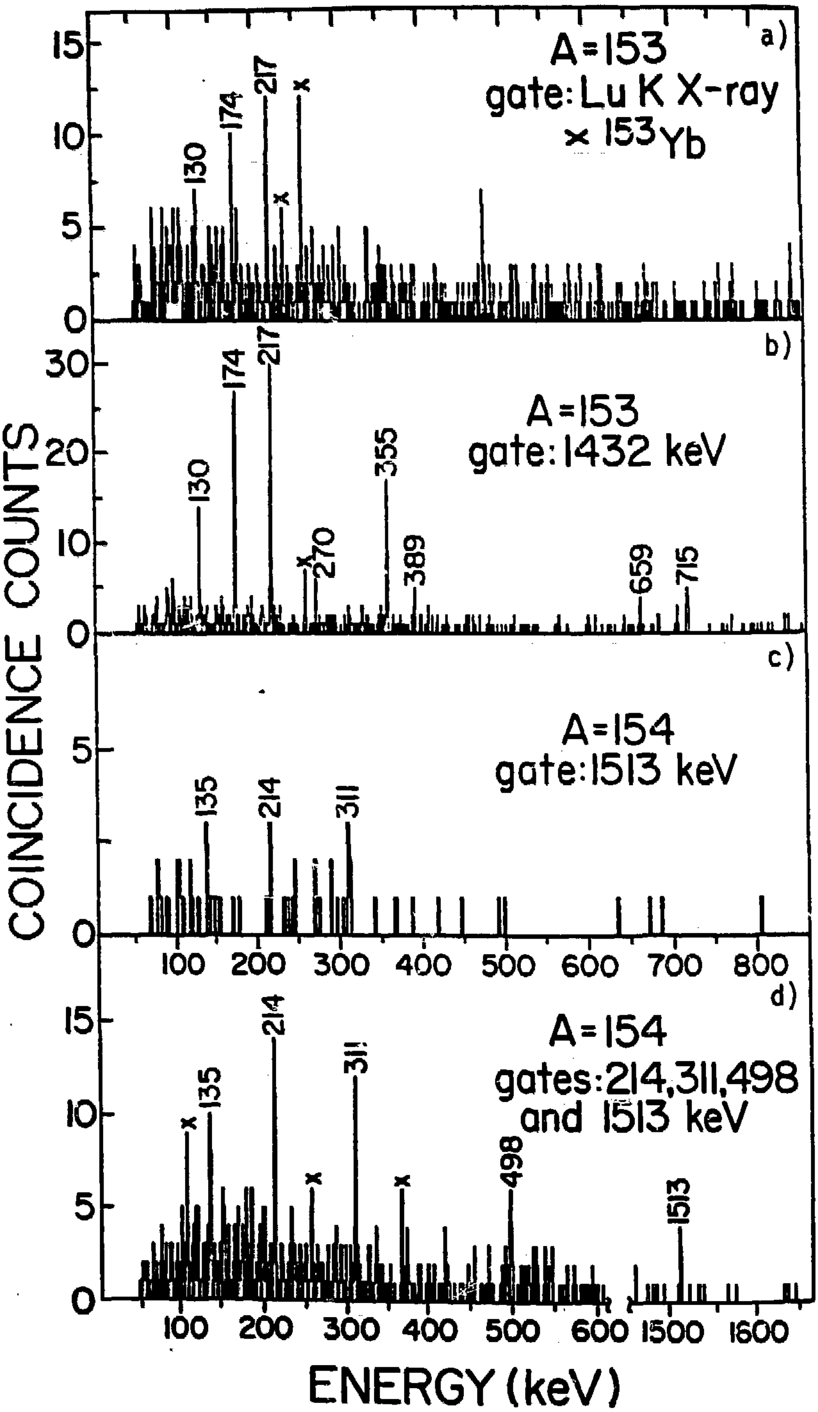

a)
A=153
gate: Lu K X-ray
× $^{153}$Yb
130
174
217
x
b)
A=153
gate: 1432 keV
130
174
217
270
355
389
659
715
c)
A=154
gate: 1513 keV
135
214
311
d)
A=154
gates: 214, 311, 498
and 1513 keV
135
214
311
498
1513
COINCIDENCE COUNTS
ENERGY (keV)

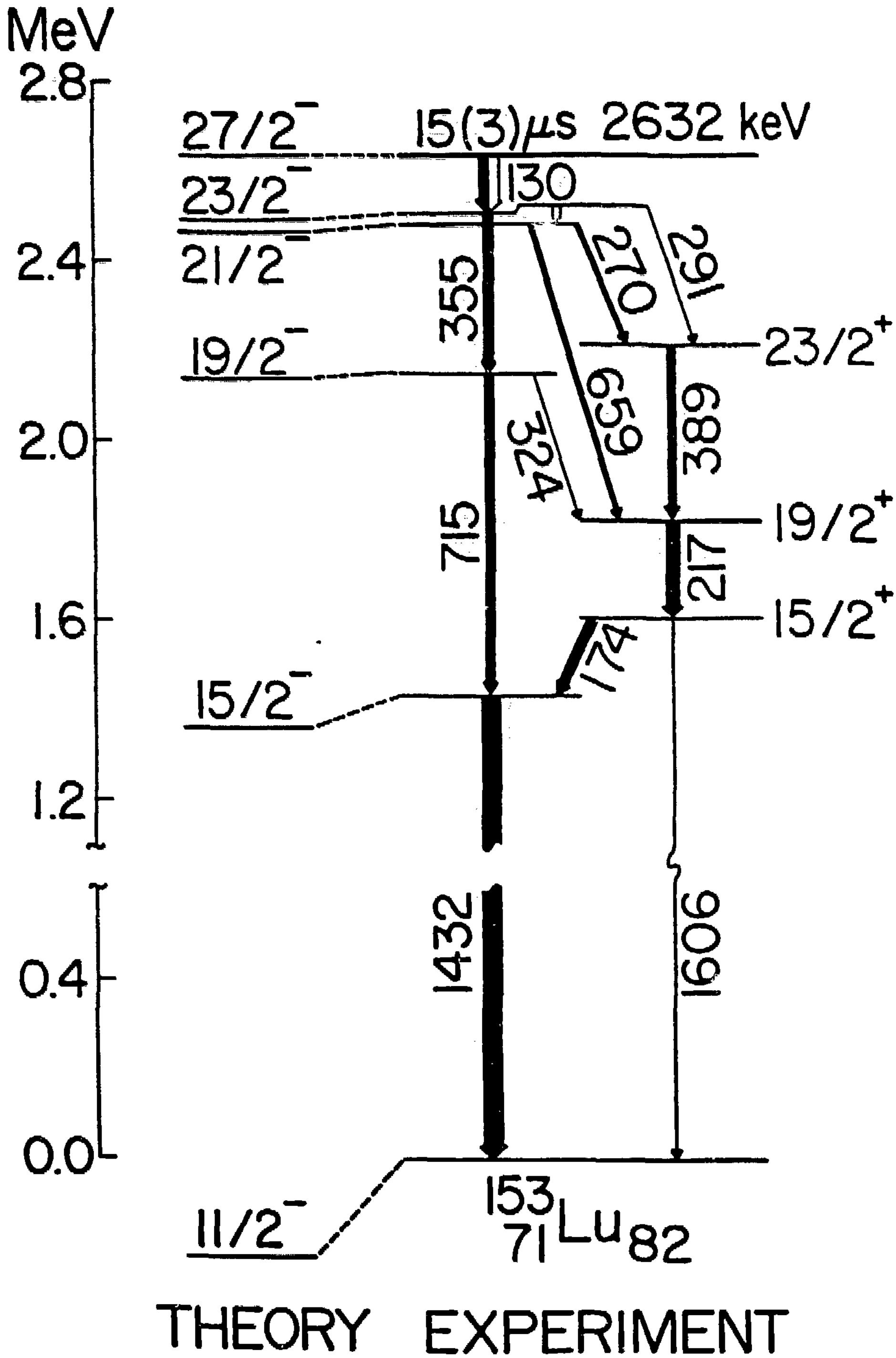
MeV
2.8
2.4
2.0
1.6
1.2
0.4
0.0
27/2⁻
23/2⁻
21/2⁻
19/2⁻
15/2⁻
11/2⁻
15(3)μs 2632 keV
130
355
270
291
659
389
324
715
217
174
1432
1606
23/2⁺
19/2⁺
15/2⁺
153
71
Lu
82
THEORY
EXPERIMENT

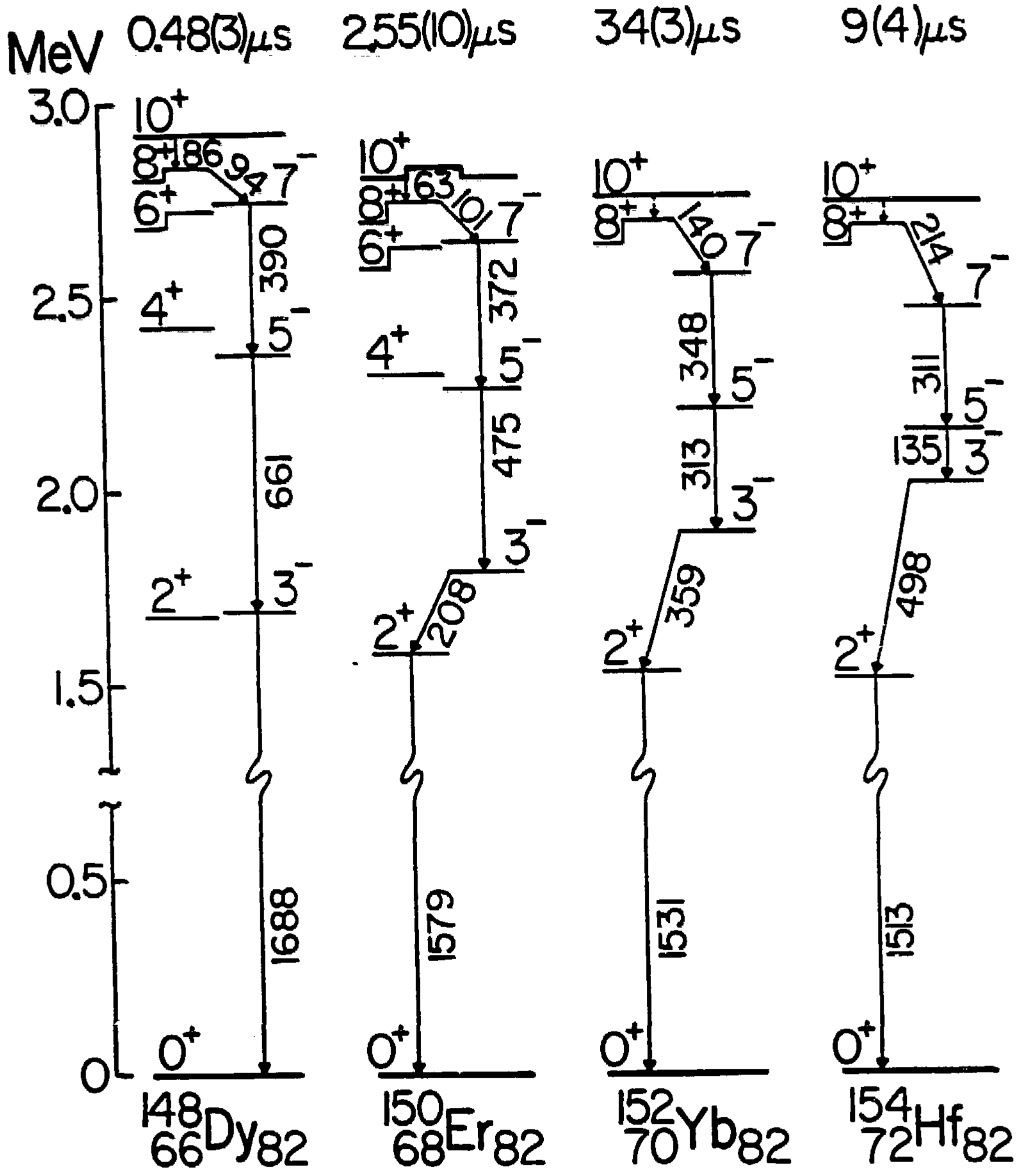

MeV
0.48(3)μs
2.55(10)μs
34(3)μs
9(4)μs
3.0
2.5
2.0
1.5
0.5
0
10+
8+
6+
7−
4+
5−
3−
2+
0+
186
94
390
661
1688
163
101
372
475
208
1579
140
348
313
359
1531
214
311
135
498
1513
148 66 Dy 82
150 68 Er 82
152 70 Yb 82
154 72 Hf 82

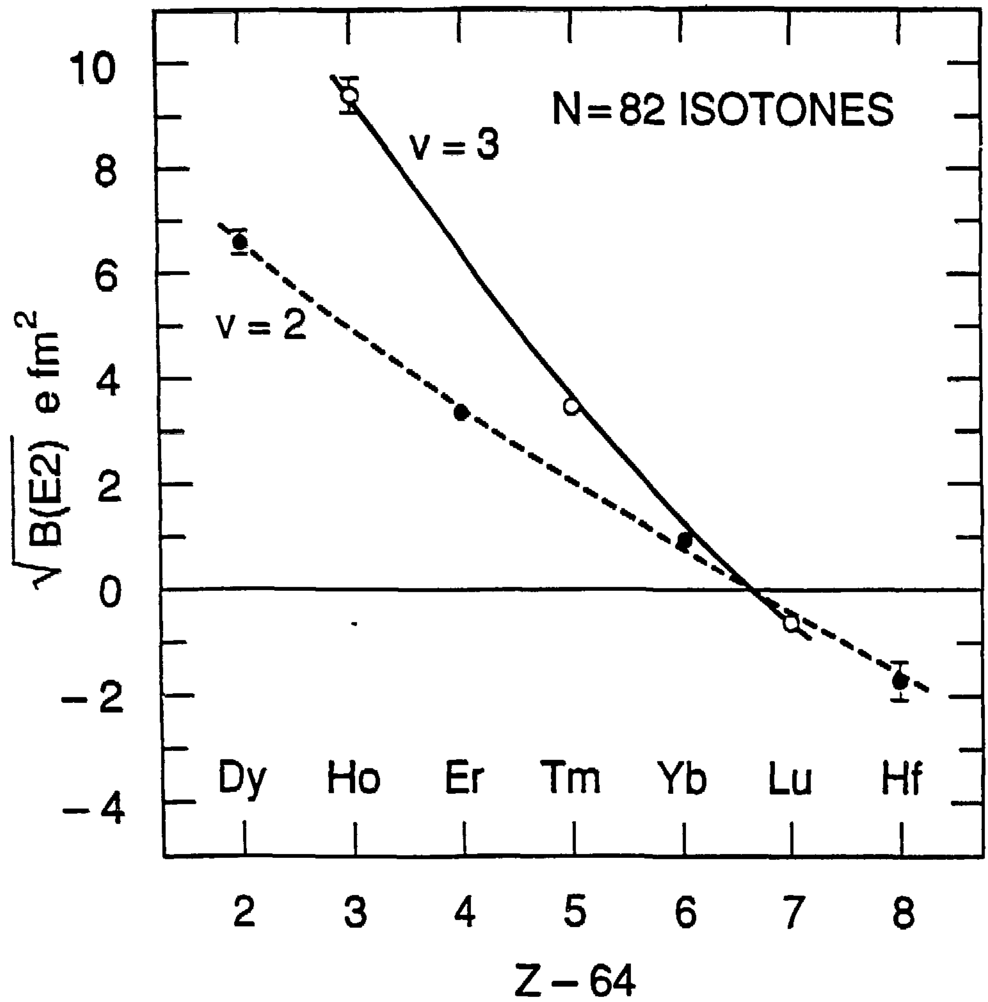
N=82 ISOTONES
v = 3
v = 2
$\sqrt{B(E2)}$ e fm$^2$
10
8
6
4
2
0
-2
-4
Dy
Ho
Er
Tm
Yb
Lu
Hf
2
3
4
5
6
7
8
Z - 64

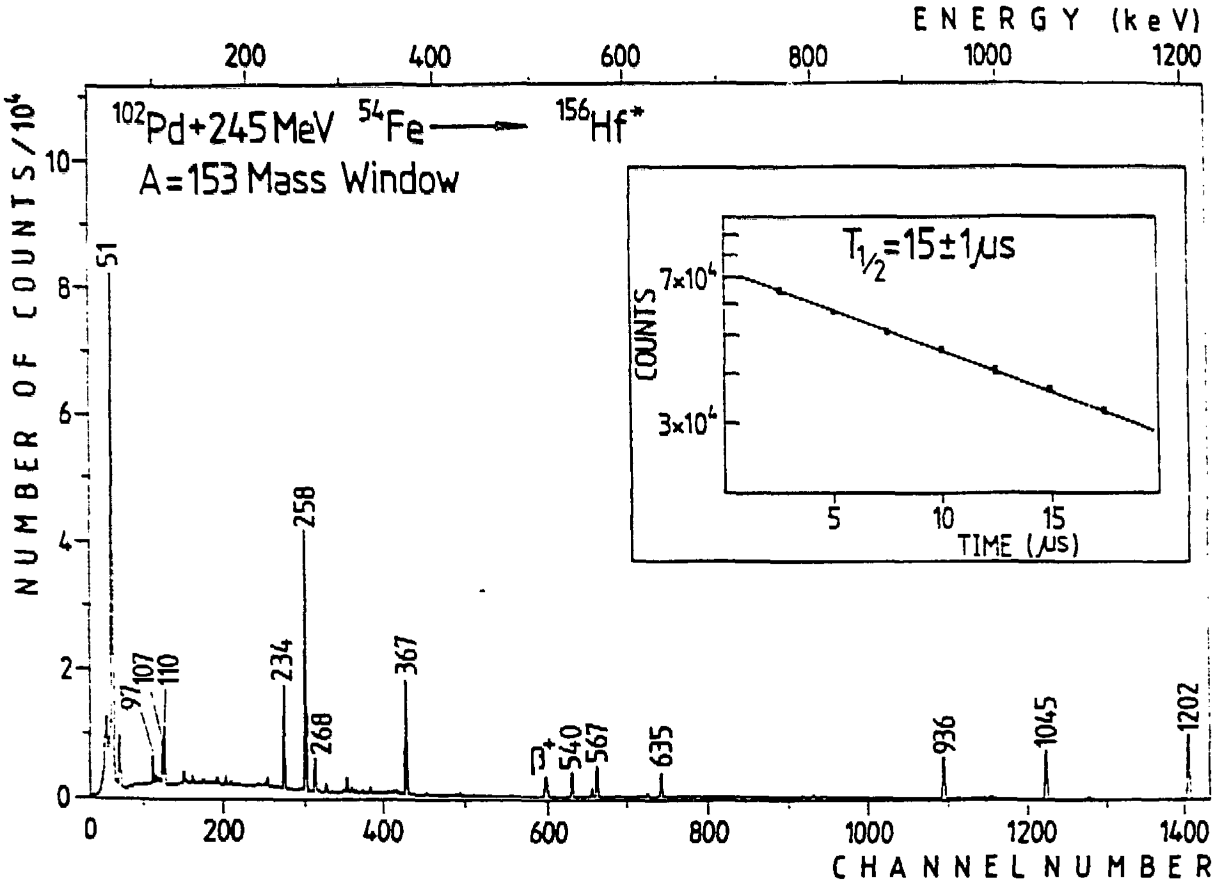

ENERGY (keV)
200
400
600
800
1000
1200
$^{102}$Pd+245 MeV $^{54}$Fe → $^{156}$Hf*
A=153 Mass Window
NUMBER OF COUNTS/10$^4$
10
8
6
4
2
0
51
97
107
110
234
258
268
367
β+
540
567
635
936
1045
1202
T$_{1/2}$=15±1μs
7×10$^4$
3×10$^4$
COUNTS
5
10
15
TIME (μs)
0
200
400
600
800
1000
1200
1400
CHANNEL NUMBER

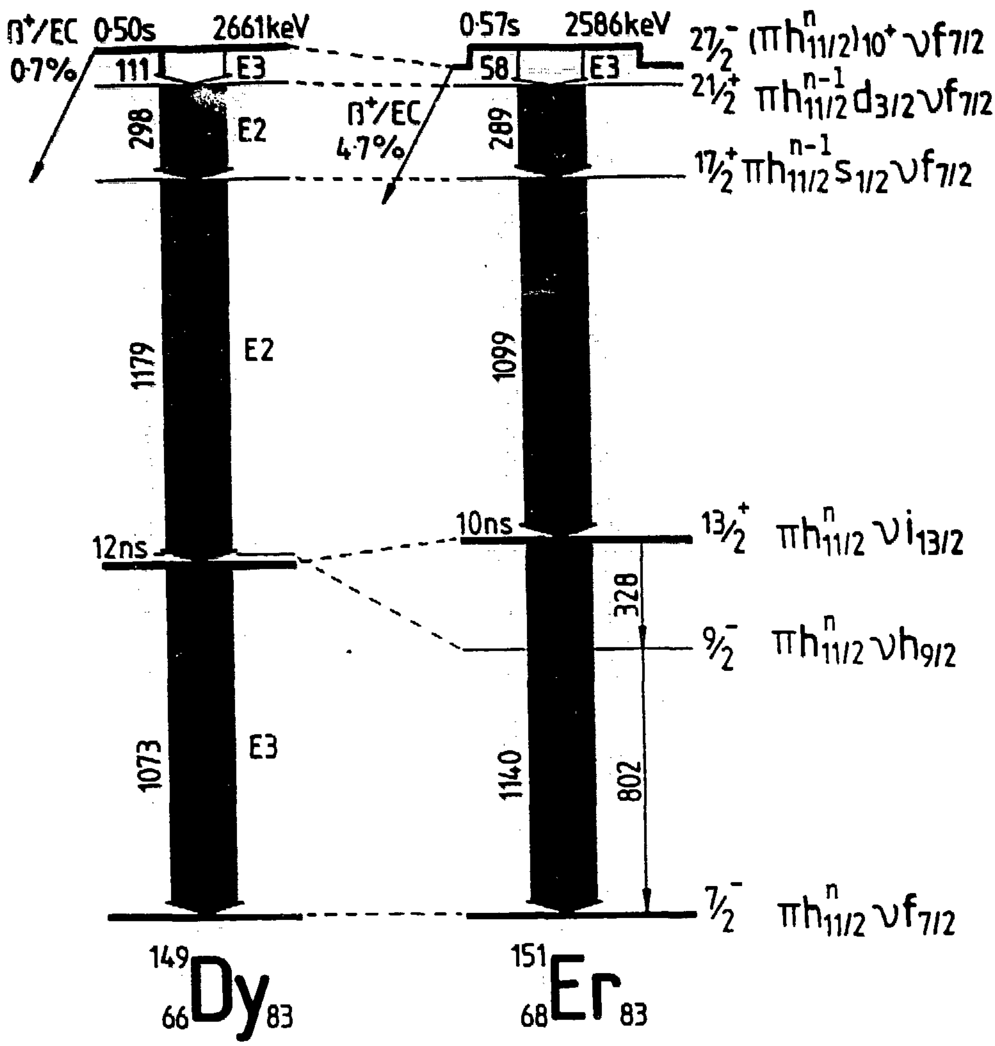

β+/EC 0·50s 2661keV
0·7%
111 E3
298 E2
1179 E2
12ns
1073 E3
149 66 Dy 83
0·57s 2586keV
58 E3
β+/EC 4·7%
289
1099
10ns
328
1140
802
151 68 Er 83
27/2⁻ (πh11/2 n)10⁺ νf7/2
21/2⁺ πh11/2 n-1 d3/2 νf7/2
17/2⁺ πh11/2 n-1 s1/2 νf7/2
13/2⁺ πh11/2 n νi13/2
9/2⁻ πh11/2 n νh9/2
7/2⁻ πh11/2 n νf7/2

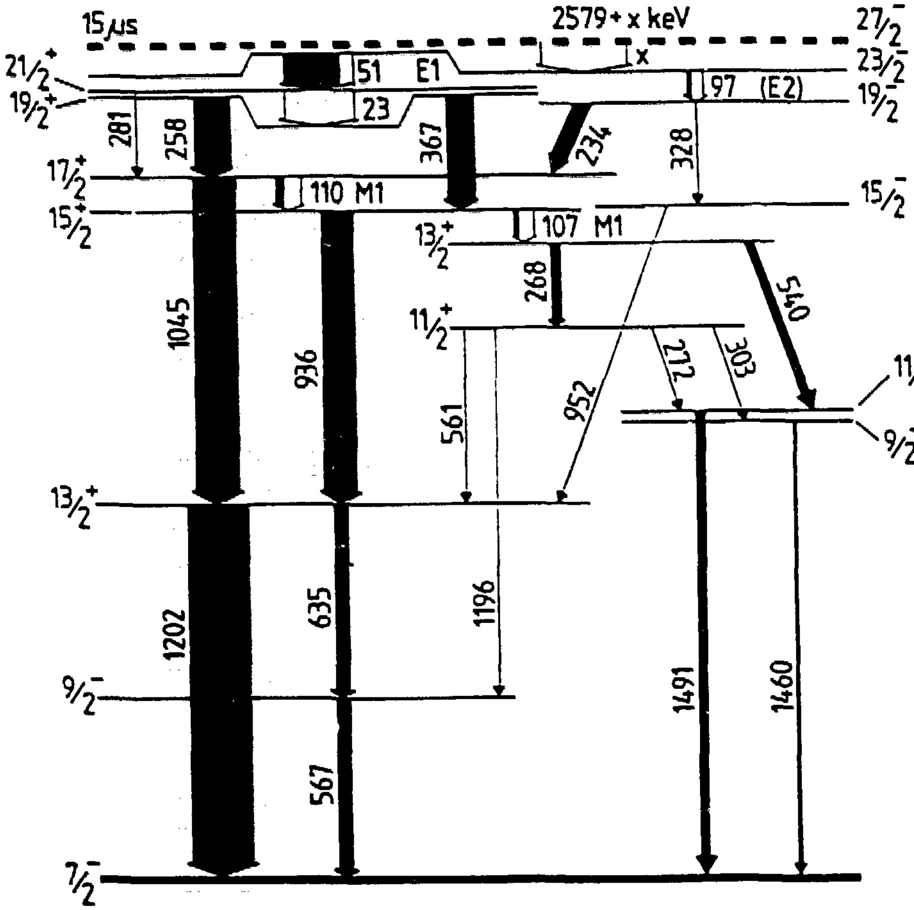
15 μs
2579 + x keV
27/2⁻
21/2⁺
19/2⁺
23/2⁻
19/2⁻
51 E1
23
x
97 (E2)
281
258
367
234
328
17/2⁺
15/2⁺
15/2⁻
110 M1
107 M1
13/2⁺
268
540
11/2⁺
272
303
11/2⁻
9/2⁻
1045
936
561
952
13/2⁺
1202
635
1196
1491
1460
9/2⁻
567
7/2⁻

$^{153}_{70}Yb_{83}$

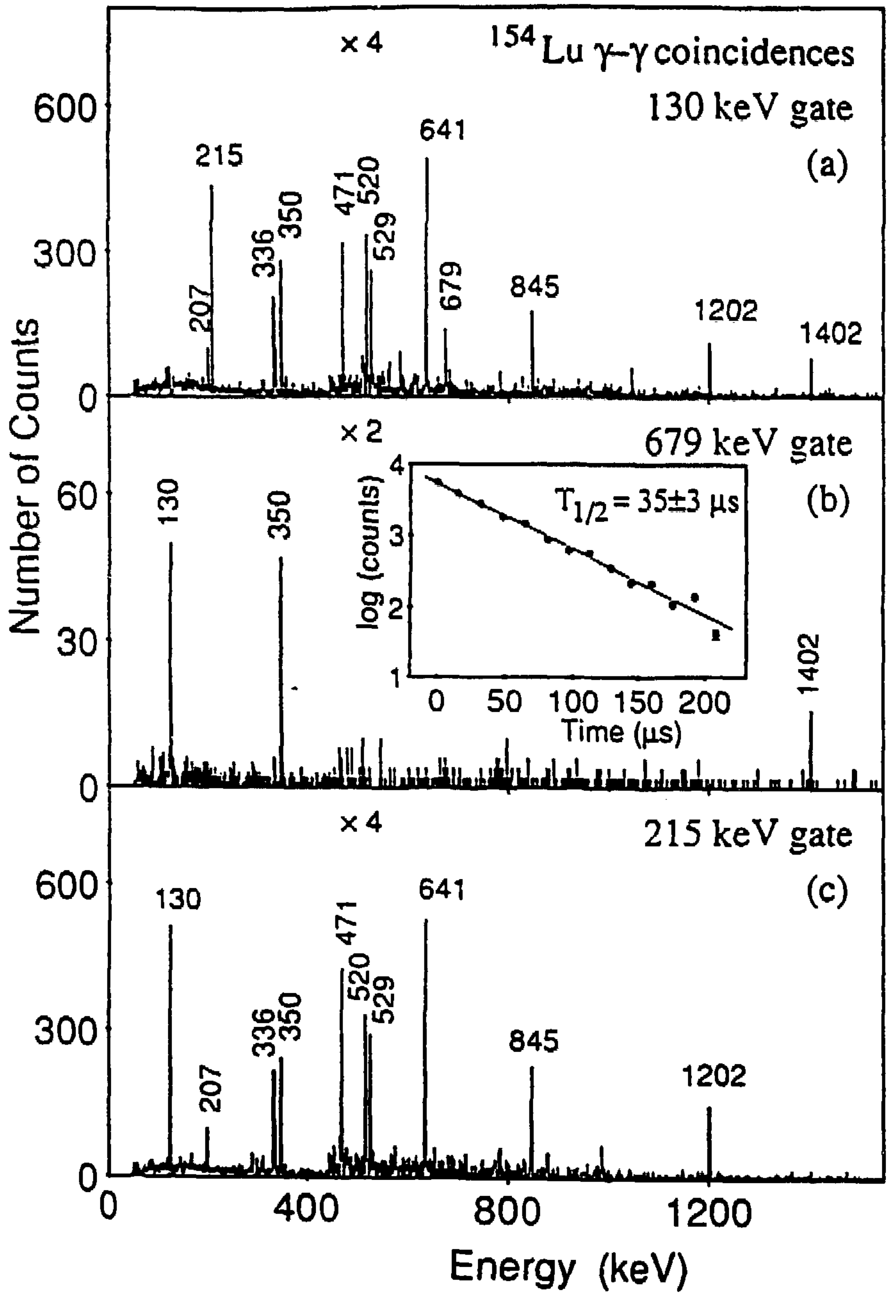

154Lu γ-γ coincidences
130 keV gate
(a)
× 4
215
207
336
350
471
520
529
641
679
845
1202
1402
679 keV gate
(b)
× 2
130
350
1402
T1/2 = 35±3 μs
log (counts)
Time (μs)
215 keV gate
(c)
× 4
130
207
336
350
471
520
529
641
845
1202
Number of Counts
Energy (keV)

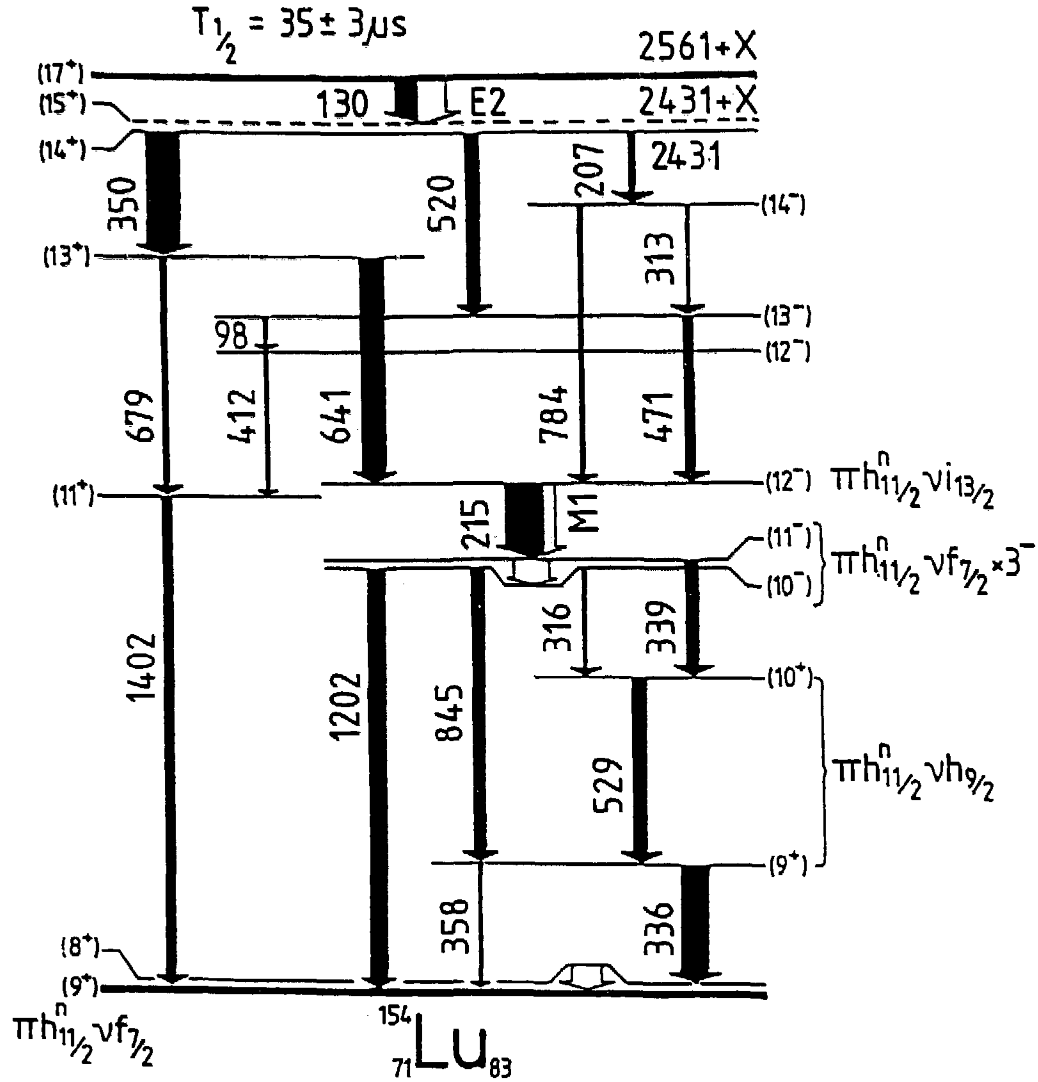
T1/2 = 35± 3μs
2561+X
(17+)
(15+)
130
E2
2431+X
(14+)
350
520
207
2431
(14−)
313
(13+)
(13−)
98
(12−)
679
412
641
784
471
(11+)
(12−) πh n 11/2 νi13/2
215
M1
(11−)
(10−)
πh n 11/2 νf7/2 ×3−
316
339
1402
1202
845
(10+)
529
πh n 11/2 νh9/2
(9+)
358
336
(8+)
(9+)
πh n 11/2 νf7/2
154 71 Lu 83

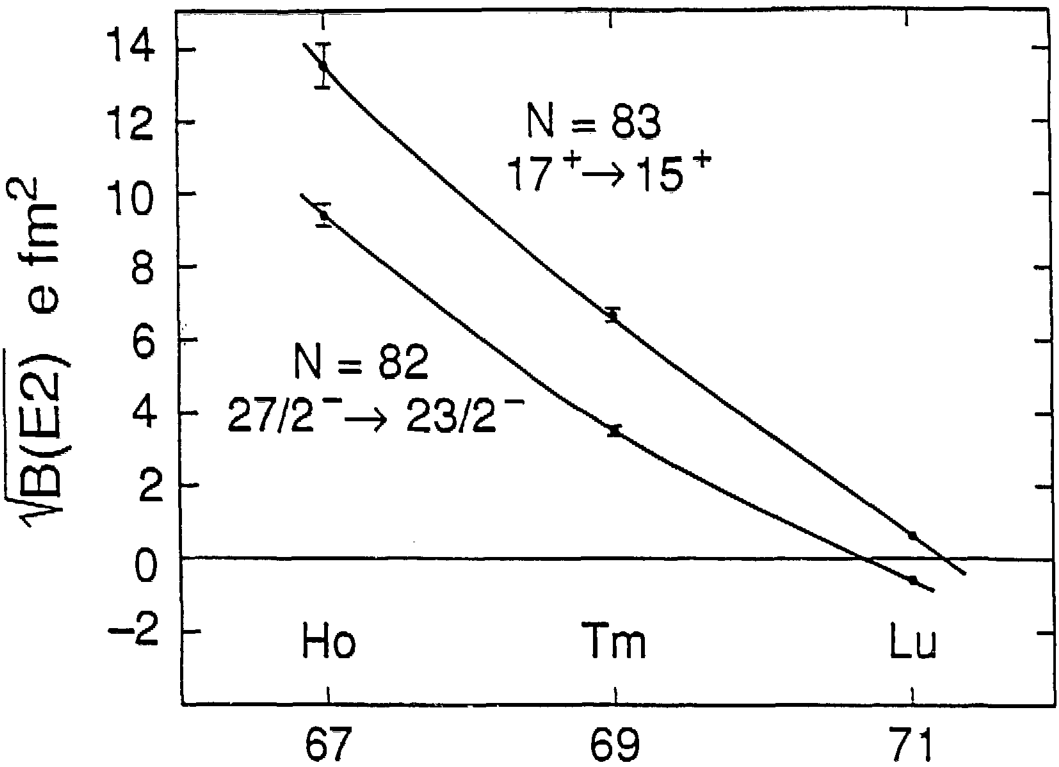

14
12
10
8
6
4
2
0
−2
$\sqrt{B(E2)}$ e fm$^2$
N = 83
17$^+$ → 15$^+$
N = 82
27/2$^-$ → 23/2$^-$
Ho
Tm
Lu
67
69
71